

Potential Advantage of Preoperative Three-Dimensional Mapping of Sentinel Nodes in Breast Cancer by a Hybrid Single Photon Emission CT (SPECT)/CT System.

Mutsuko Ibusuki¹, Yutaka Yamamoto¹, Teru Kawasoe¹, Shinya Shiraishi²,
Seiji Tomiguchi², Yasuyuki Yamashita², Yumi Honda³, Kenichi Iyama³,
Hirotaka Iwase¹

¹Department of Breast and Endocrine Surgery, Graduate School of Medical Sciences,
Kumamoto University, 1-1-1 Honjo Kumamoto, Kumamoto, 860-8556, Japan

²Department of Diagnostic Radiology, Graduate School of Medical Sciences,
Kumamoto University

³ Department of Surgical Pathology, Graduate School of Medical Sciences,
Kumamoto University

Corresponding author & Reprints

Yutaka Yamamoto, M.D., PhD.

The Department of Breast and Endocrine Surgery, Graduate School of Medical
Sciences, Kumamoto University, 1-1-1 Honjo, Kumamoto, Kumamoto, 860-8556,
Japan

Tel 81-96-373-5521, Fax 81-96-373-5525

E-Mail: ys-yama@triton.ocn.ne.jp

Abstract

Objective: This study aims to assess the role of three dimensional single-photon emission computed tomography (3D-SPECT/CT) in sentinel node (SN) identification, and to analyze the impact of such information on estimating metastases to SNs.

Background: Nodal status is a key factor for breast cancer. SN biopsy has been established as the alternative to routine axillary dissection these days. We investigated both the anatomical location of SNs demonstrated by our 3D-SPECT/CT system and the correlation to SN positivity.

Methods: Two hundred and twenty-three clinically node-negative patients underwent SN biopsy. All of the axillary structures, including SNs, were visualized by a SPECT/CT combined system after subcutaneous injection of ^{99m}Tc -phytate. By plotting the visualized SNs, the most frequent SN location 'Pedestal area (PA)' was designated.

Results: SPECT/CT detected ^{99m}Tc uptake in 217 cases (97.3%). 3D-SPECT/CT images visualized the accurate location of SNs in each case. In patients whose SNs were histopathologically negative (SN-), 228 (98.3%) SNs were found in the PA, and 4 (1.7%) were in other zones. In those with histopathologically positive SNs (SN+), 65 (78.3%) SNs were in the PA and 18 (21.7%) were outside it. The difference in SN distribution (i.e., in or out of the PA) between SN+ and SN- patients was statistically significant ($p < 0.001$, chi-square test).

Conclusions: SN biopsy navigated by 3D-SPECT/CT can clarify the preoperative anatomical localization of SNs in patients with breast cancer. Atypical distribution of SNs out of the PA may suggest SN positivity, reflecting failure of the lymphatic drainage systems.

Key words : Sentinel Node Mapping, Breast cancer, 3D-SPECT/CT, metastases

INTRODUCTION

Sentinel node biopsy has largely replaced axillary clearance in the nodal staging in breast cancer. To search for SNs, injection of blue dye or radiotracer or both are commonly used. In the radiotracer procedure, presurgical lymphatic mapping has been helpful because the lymphatic drainage patterns are unpredictable and variable for each patient, even those with tumors in the same breast region (1). But it is difficult to determine the exact anatomic location of the detected nodes with planar imaging.

Recently, a hybrid imaging device consisting of a single photon emission CT (SPECT) and a low dose CT installed on the same platform (SPECT/CT) has been introduced. SN detection by SPECT/CT has been reported in a few papers on breast cancer(2-6) as well as other cancers: malignant melanoma (7), head and neck carcinoma(8), bladder and prostate cancer(9, 10)(11), cervical cancer(12), and lung cancer(13). Most of these indicate that SPECT/CT imaging improves the anatomic localization and identification of SNs. We are using a multi-detector CT, which generates correctly fused 3D images from a single examination and provides amazing stereographic localization of SNs. Each modality is commercially available, examination room which is large enough to install two equipments and a workstation to fuse two series of images are required. It takes only more 5 minutes to acquire the images by multi-detector CT following after usual 30-min SPECT imaging. Although additional charge for CT and exposure to radiation would be worried about, high quality imaging and precise treatment can wipe out these concerns.

In this study, we introduce our experiences that allow more accurate preoperative localization of SNs, and also report the helpful information provided by 3D-SPECT/CT on existence of metastases to the lymphnodes.

PATIENTS and METHODS

Patients

From July 2002 to November 2006, 223 patients with biopsy-proven breast cancer (Tumor size <5cm) and clinically negative axilla were enrolled in this study. Informed consent was obtained from all patients according to the regulations of our institution. Patients with multicentric tumors, subareolar and inflammatory tumors, or metastatic breast cancer, and those receiving neoadjuvant chemotherapy or lumpectomy, were excluded.

System design

We used a combined SPECT/CT system incorporating a commercially available gantry-free SPECT with dual-head detectors (Skylight, ADAC Laboratories, Milpitas, CA, USA) and an eight multidetector-row CT scanner (Light-speed Ultra Instrument, GE, Milwaukee, WI, USA). The two instruments were juxtaposed so that the CT table bearing the patient could be moved directly into the SPECT scanner before CT scanning. Consequently, each patient was positioned identically for SPECT and CT imaging.

Lymphoscintigraphy

All patients underwent lymphoscintigraphy on the day before surgery using 37Mbc of technetium Tc 99m (^{99m}Tc)-phytate (DAI-ICHI Radioisotope Laboratories, Tokyo, Japan). The radioactive tracer was injected subcutaneously for half dose and peritumorally for the rest. Lymphoscintigraphy was then performed with the SPECT dual-head detectors imaging one frame every 60 seconds for 30 minutes to identify focal

areas of accumulation, followed by multiple 5-min static images. In all patients, delayed images were obtained 2 and a half hour after first imaging.

Single-photon-emission computed tomography/ computed tomography imaging

SPECT was performed 3 hours after the administration of radiotracer for each patient. Data were acquired with a vertex general-purpose parallel-hole (VXGP) collimator. A 360° SPECT scan encompassing the thorax and upper abdomen was acquired. Computed tomography images were obtained without contrast administration. Reconstructed CT images were processed into Digital Imaging and Communications in Medicine (DICOM) data and then transferred to Pegasys (ADAC Laboratories, Milpitas, CA, USA), a workstation for SPECT processing. One lumen of a three-way stopcock (inner diameter 4mm, length 10mm) containing an aqueous solution of Tc-phytate and a contrast medium was used as an external fiducial marker. To obtain a precise record of both images, these markers were fixed to the common platform for SPECT and CT imaging. The two scans were performed sequentially, and the resulting images were fused by manually aligning the external fiducial markers in the two images on a workstation operated by an experienced radiologist.

Using our 3D-SPECT/CT system, fusion images show quite accurate localization of SNs stereographically. Multiple side views from various angles and exact body layer images are obtained (Fig.1a and Fig. 1b). By capturing images of the appropriate layer of the body, anatomical relationships between each SN and other structures such as vessels, muscles, ribs, and the ipsilateral nipple can be understood clearly in advance of surgery (Fig.2).

Surgery

A hand-held gamma probe (Crystal CXS-SG03; Anzai Medical, Tokyo, Japan) was used for measuring radioactivity, and counts were accumulated for every 10 seconds and recorded. Sentinel lymph nodes showed focal uptake of radiotracer to 10 times the background count rate. Intraoperative SN mapping was also performed with 2ml of 1% patent blue dye subcutaneously injected above the tumor before incision.

SNs were resected under general anesthesia in patients undergoing simultaneous resection of primary tumor. When resection of the SNs was performed for axillary node staging only, local anesthesia was used. If the SNs were positive, patients received level I and II axillary lymph node dissection or neoadjuvant chemotherapy according to the therapeutic protocol of our institution. Supraclavicular and parasternal LN biopsies were not routinely performed.

Pathological examination

In cases of simultaneous resection with primary tumor, SNs were examined intraoperatively as 2-mm frozen sections. After surgery, the SNs were fixed in 10% buffered formalin, processed overnight, and serially sectioned into ~2-mm slices, which were embedded in paraffin and re-evaluated histopathologically using routine hematoxylin-eosin staining. SNs removed for axillary staging were formalin-fixed, sectioned, processed and evaluated in the same manner.

Statistical analysis

Statistical comparisons between the groups were done using the Pearson χ^2 test as implemented in the JMP statistical software package, Japanese version 4.0 (SAS). P values $<.05$ were considered as statistically significant.

RESULTS

Patient characteristics

The baseline characteristics of the enrolled patients are indicated in Table 1. 167 patients (74.8%) were node-negative, and 57 (25.2%) were node-positive according to the final histological reports. Tumor size was significantly larger for node-positive than node-negative patients ($p=0.0026$). Gender, age, kind of operation, and tumor location had no significant correlation with nodal status.

The number of hot spots and the detection rate

The numbers of nodes showing radiotracer uptake detected by SPECT/CT imaging are shown in Table 2. The average number of "hot" SNs was 1.40 ± 0.053 in the node-negative group, 1.46 ± 0.091 in the node-positive group (no significant difference). The detection rate was 97.3%; SNs were clearly visualized in 217 of 223 patients. In the remaining 6 patients no nodal uptake could be detected by SPECT/CT, but SN detection and biopsy was accomplished by complementary use of blue dye and intraoperative gamma probe. A significantly ($p=0.029$) higher percentage of negative scintigraphy was observed in the node-positive group (7.1%) than in the node-negative group (1.2%).

SN mapping and Distribution of SNs

Among the 217 patients in whom hot nodes were detected by 3D-SPECT/CT, the location of these nodes was categorized according to our original SN grouping map (Fig.3a). This map was devised from the classification of regional lymph nodes developed by the Japanese Society of Clinical Oncology(14). In this mapping, the

axillary region is divided into 4 parts based on the anatomical relationships between the SNs and axillary vessels (axillary vein, lateral thoracic vein, and dorsal thoracic vein.) The brachial zone, as shown in Fig. 2, is at the top of the axilla, adjacent to the axillary vein. The rest of the axilla is separated into 3 parts by the lateral and dorsal thoracic veins. In dorsal-to-ventral order, these 3 parts are named the pectoral, central, and subscapular zones. Nodes in the 4 axillary zones (brachial, pectoral, central, subscapular) are more clearly visualized by 3D images than planar images. The subpectoral zone (Fig. 3b), parasternal zone (Fig. 3c), interpectoral zone (Fig. 3d) and infraclavicular zone are depicted accurately by planar SPECT/CT images. For each patient, all the SNs detected as hot spots were categorized and plotted in their respective zones by the most informative image of each zone.

In most cases, SNs were located in the pectoral, central, or subscapular zones. Furthermore, the most frequent location was the upper part of these 3 zones, which form a trapezoidal area. We designated this area as the “Pedestal Area” (PA). PA is explained as the area, shaped like a triangle with its apex removed, bounded by the lateral edge of the major pectoral muscle, the anterior edge of the dorsal thoracic muscle, and a horizontal line drawn at half height between the axillary vein and ipsilateral nipple.

The total number of SNs imaged by 3D-SPECT/CT was 305. Table 3 shows the number of hot spots inside and outside the PA. In the node-negative group, 228 (98.3%) were found in the PA, and only 4 (1.7%) were outside it. In contrast, in the node-positive group 65 (78.3%) were in the PA and 18 (21.7%) were outside it, most frequently in the brachial zone. The difference in SN distribution (in vs. out of the PA) between node-

positive and node-negative patients was statistically significant ($p < 0.001$). Fig. 4 indicates the distribution of SNs detected as hot spots by 3D-SPECT/CT.

DISCUSSION

SN biopsy is a safe and accurate method of screening the axillary nodes for metastasis in early stage breast cancer (15). We analyzed three-dimensional SPECT/CT images that visualized the stereographical location of the SNs. Prior to biopsy, we always simulate the site of incision and the size and depth of the SNs by combining information. This simulation facilitates pinpoint biopsy of the SNs, thus we apply our procedure at the outset to investigate nodal status for determining therapeutic plan of the patients who may need neoadjuvant systemic therapy.

Lerman et al. compared the usefulness of SPECT-CT and planar images for the preoperative localization of draining nodes in 157 consecutive patients with breast cancer(3). They suggest SPECT/CT can detect hot nodes that planar imaging misses due to scattered radiation from the injection site, generally called “shine through.” They also show that SPECT/CT significantly identified hot parasternal nodes missed on planar images, and can exclude sites of false-positive nonnodal uptake. They subsequently reported SPECT/CT improved SN identification in overweight patients with breast cancer(4). Their success rate of SN detection by SPECT-CT was 90% and mean number of hot nodes was 2.2 ± 1.8 per patient. Our detection rate of 97.3% is much higher than theirs but the mean number of hot nodes of 1.42 ± 0.68 per patient is lower. Although no study has been done to compare ^{99m}Tc -phytate and ^{99m}Tc -rhenium colloid, the differences in these success rates and numbers of hot nodes may depend on a difference in the size of the radiocolloid particle. The phytate we use forms larger particles (100-1000nm) than their rhenium colloid (50-200nm), which may allow more specific accumulation in the SNs.

Ogasawara et al. reported that an increased number of hot spots visualized by planar lymphoscintigraphy was significantly correlated with metastasis (16). They reported that metastasis was found for 57.1% in patients with more than 2 nodes visualized, while 23.0% in patients with 1 node and 22.2% in patients with failure localisation had metastasis. In our study, metastasis was found for 28.4% in patients with more than 2 nodes visualized, 21.3% in patients with 1 node and 66.6% in patients with failure of localization. Moreover, the average number of hot spots did not differ significantly between the node negative and node positive groups in our study. Our results seem quite opposite to theirs. They speculate that disruption of phagocytosis by macrophages in the nodal sinus due to metastasis leads migration of the radiocolloid to other surrounding nodes. According to their speculation, low amount of radiotracer stagnates before metastatic SN, and then, excess amount of radiotracer migrates to second or other echelon node. Their injection dose of 185Mbc is 5-fold of ours. This may cause both their higher multiple visualization rates and our higher failure of localization rates. About failure of localization of SNs, the most common reasons have been reported to be technical matters (particle size, insufficient time between injection and scan), previous surgery, patient age, and obesity. In our study, all failed patients were applied to some of these conditions, over 50 years old, and one obese patient in the node-negative group. Additionally, metastatic involvement of the SN has also previously been reported to be a cause of failure of localization in up to 63% patients with negative lymphoscintigraphy(17). In our study, node positive patients showed a significantly higher rate of negative SPECT/CT (4 out of 6). This may suggest that negative SPECT/CT in current study correlates with the existence of metastasis to SNs occupied

with cancer cells.

In our results, the Pedestal Area (PA) was the most common site of the SNs detected by our mapping technique. 96.1% of hot spots (293 out of 305) were observed in this area (Fig. 4). Pavlista et al. studied the topographical location of SNs in the axillas of 12 female cadavers(18). Though they used only blue dye injected into the upper-outer quadrant of the breast, all SNs were located within a 2-cm radius from the intersection of the third intercostobrachial nerve and thoracoepigastric vein. Another study reported that 89.1% of SNs were located cranially to the intercostobrachial nerve and within 2 cm of the lateral edge of the minor pectoral muscle (19). The PA is almost as same as these reported anatomical locations, namely the cranial side of level I nodes. We found that node-positive and node-negative patients differed significantly in the occurrence of SNs outside the PA. In the case of metastasis to SN, failure of the normal lymph drainage due to occupation by cancer cells may alter the drainage route(20). Consequently a broad distribution or atypical hot spots reflecting second echelon nodes were detected. Although there are no previous reports of such detailed SN mapping, the “brachial” nodes nearest the PA can be regarded as equivalent to an upper axillary level such as level II (interpectoral, subpectoral), level III (infraclavicular), or parasternal zone, and may be worthy of attention as a predictor of axillary positivity.

In conclusion, SN biopsy navigated by 3D-SPECT/CT can provide high quality the preoperative anatomical localization of SNs in patients with breast cancer. Atypical distribution of SNs out of the PA may suggest axillary positivity as a reflection of the failure of lymphatic drainage systems. Our report is the first study putting 3D-SPECT/CT to practical use to our knowledge.

Conflict of interest statement

None declared.

Figure Legends

Fig.1 SN mapping by 3D-SPECT/CT imaging; Surface mapping (a) is useful to identify the aiming SNs by gamma probe just before surgery. Anatomical relationships between each SN and other structures of axillary region can be understood by anatomical mapping (b).

Fig.2 SN pointed out by 3D imaging; SN was clearly identified by its anatomical location and its shape and size. (Arrowhead)

Fig.3 SN mapping by 3D-SPECT/CT; mapping classification of SNs according to the relationships with surrounding structures(a), and planar SPECT/CT images of extra-axillary nodes: subpectoral node (b), parasternal node (c), interpectoral node (d)

Fig.4 Distribution of hot spots. Blue spots: node-negative group, pink spots; node-positive group. Most spots were concentrated within the “Pectoral Area.”

REFERENCES

1. Estourgie SH, Nieweg OE, Olmos RA, Rutgers EJ, Kroon BB. Lymphatic drainage patterns from the breast. *Ann Surg* 2004; 239: 232-7.
2. Husarik DB, Steinert HC. Single-photon emission computed tomography/computed tomography for sentinel node mapping in breast cancer. *Semin Nucl Med* 2007; 37: 29-33.
3. Lerman H, Metser U, Lievshitz G, Sperber F, Shneebaum S, Even-Sapir E. Lymphoscintigraphic sentinel node identification in patients with breast cancer: the role of SPECT-CT. *Eur J Nucl Med Mol Imaging* 2006; 33: 329-37.
4. Lerman H, Lievshitz G, Zak O, Metser U, Schneebaum S, Even-Sapir E. Improved sentinel node identification by SPECT/CT in overweight patients with breast cancer. *J Nucl Med* 2007; 48: 201-6.
5. Gallowitsch HJ, Kraschl P, Igerc I, et al. Sentinel node SPECT-CT in breast cancer. Can we expect any additional and clinically relevant information? *Nuklearmedizin* 2007; 46: 252-6.
6. van der Ploeg IM, Valdes Olmos RA, Nieweg OE, Rutgers EJ, Kroon BB, Hoefnagel CA. The additional value of SPECT/CT in lymphatic mapping in breast cancer and melanoma. *J Nucl Med* 2007; 48: 1756-60.

7. Ishihara T, Kaguchi A, Matsushita S, et al. Management of sentinel lymph nodes in malignant skin tumors using dynamic lymphoscintigraphy and the single-photon-emission computed tomography/computed tomography combined system. *Int J Clin Oncol* 2006; 11: 214-20.
8. Wagner A, Schicho K, Glaser C, et al. SPECT-CT for topographic mapping of sentinel lymph nodes prior to gamma probe-guided biopsy in head and neck squamous cell carcinoma. *J Craniomaxillofac Surg* 2004; 32: 343-9.
9. Kizu H, Takayama T, Fukuda M, et al. Fusion of SPECT and multidetector CT images for accurate localization of pelvic sentinel lymph nodes in prostate cancer patients. *J Nucl Med Technol* 2005; 33: 78-82.
10. Sherif A, Garske U, de la Torre M, Thorn M. Hybrid SPECT-CT: an additional technique for sentinel node detection of patients with invasive bladder cancer. *Eur Urol* 2006; 50: 83-91.
11. Krenqli M, Ballare A, Cannillo B, et al. Potential advantage of studying the lymphatic drainage by sentinel node technique and SPECT-CT image fusion for pelvic irradiation of prostate cancer. *Int J Radiat Oncol Biol Phys* 2006; 66: 1100-4.
12. Zhang WJ, Zheng R, Wu LY, Li XG, Li B, Chen SZ. [Clinical application of sentinel lymph node detection to early stage cervical cancer]. *Ai Zheng* 2006; 25: 224-8.

13. Nomori H, Ikeda K, Mori T, et al. Sentinel node identification in clinical stage Ia non-small cell lung cancer by a combined single photon emission computed tomography/computed tomography system. *J Thorac Cardiovasc Surg* 2007; 134: 182-7.
14. JSCO. Classification of Regional Lymph Nodes in Japan. *International Journal of Clinical Oncology* 2003; vol.8
15. Veronesi U, Paganelli G, Viale G, et al. A randomized comparison of sentinel-node biopsy with routine axillary dissection in breast cancer. *N Engl J Med* 2003; 349: 546-53.
16. Ogasawara Y, Yoshitomi S, Sato S, Doihara H. Clinical Significance of Preoperative Lymphoscintigraphy for Sentinel Lymph Node Biopsy in Breast Cancer. *J Surg Res* 2007.
17. Brenot-Rossi I, Houvenaeghel G, Jacquemier J, et al. Nonvisualization of axillary sentinel node during lymphoscintigraphy: is there a pathologic significance in breast cancer? *J Nucl Med* 2003; 44: 1232-7.
18. Pavlista D, Eliska O, Duskova M, Zikan M, Cibula D. Localization of the sentinel node of the upper outer breast quadrant in the axillary quadrants. *Ann Surg Oncol* 2007; 14: 633-7.
19. Motomura K, Inaji H, Komoike Y, et al. Sentinel Node Biopsy in Breast Cancer Patients with Clinically Negative Lymph-Nodes. *Breast Cancer* 1999; 6: 259-62.

20. Guenther JM, Krishnamoorthy M, Tan LR. Sentinel lymphadenectomy for breast cancer in a community managed care setting. *Cancer J Sci Am* 1997; 3: 336-40.

Tables:

Table 1. patient characteristics

	Total	Node negative	Node positive	<i>p</i> value
	223	167(74.8%)	56(25.2%)	
Female:Male	222:1	167:0	55:1	
Age(Median)	58	59	57	<i>p</i> =0.23
(Min-Max)	(30-81)	(30-81)	(30-80)	
Op BCT	118(69.0%)	91(77.1%)	35(66.0%)	
Mastectomy	53(31.0%)	27(22.9%)	18(34.0%)	<i>p</i> =0.13
SNB only	52	49	3	
Tumor Size				
(Median;mm)	17	15	20	<i>p</i> =0.0026
(Min-Max)	(3-50)	(3-50)	(8-50)	
Location U-O	100(44.8%)	67(40.1%)	33(58.9%)	
(N / %) L-O	29(13.0%)	22(13.2%)	7(12.5%)	
U-I	69(30.9%)	58(34.7%)	11(19.6%)	
L-I	10(4.4%)	9(5.4%)	1(1.8%)	
Central	13(5.8%)	9(5.4%)	4(7.1%)	<i>p</i> =0.095

Abbreviations; BCT:breast conserving therapy, SNB: sentinel node biopsy,
U-O:upper-outer, L-O: lower outer, U-I: upper inner, L-I:lower inner

Table 2. The number of hot nodes by SPECT/CT

Number of Hot nodes	Total	Node negative	Node positive
0	6(2.6)	2(1.2)*	4(7.1)*
1	136(60.7)	107(64.0)	29(51.7)
2	64(28.7)	48(28.7)	16(28.6)
3	16(7.1)	9(5.4)	7(12.5)
4	1(0.4)	1(0.6)	0(0)
Average \pm SD	1.42 \pm 0.68	1.40 \pm 0.05	1.46 \pm 0.09
Success of SN detection case (%)	217(97.3%)	165(98.8%)	52(92.9%)

*p=0.0026

Table 3. Number of hot nodes in or out of “Pedestal area”

Number of Hot nodes	Node negative	Node positive
Pedestal Area	228(98.3%)	65(78.3%)
Others	4(1.7%)	18(21.7%) $p<0.001$
brachial	2	11
parasternal	1	3
infraclavicular	1	1
interpectoral	0	1
subpectoral	0	2

Fig.1

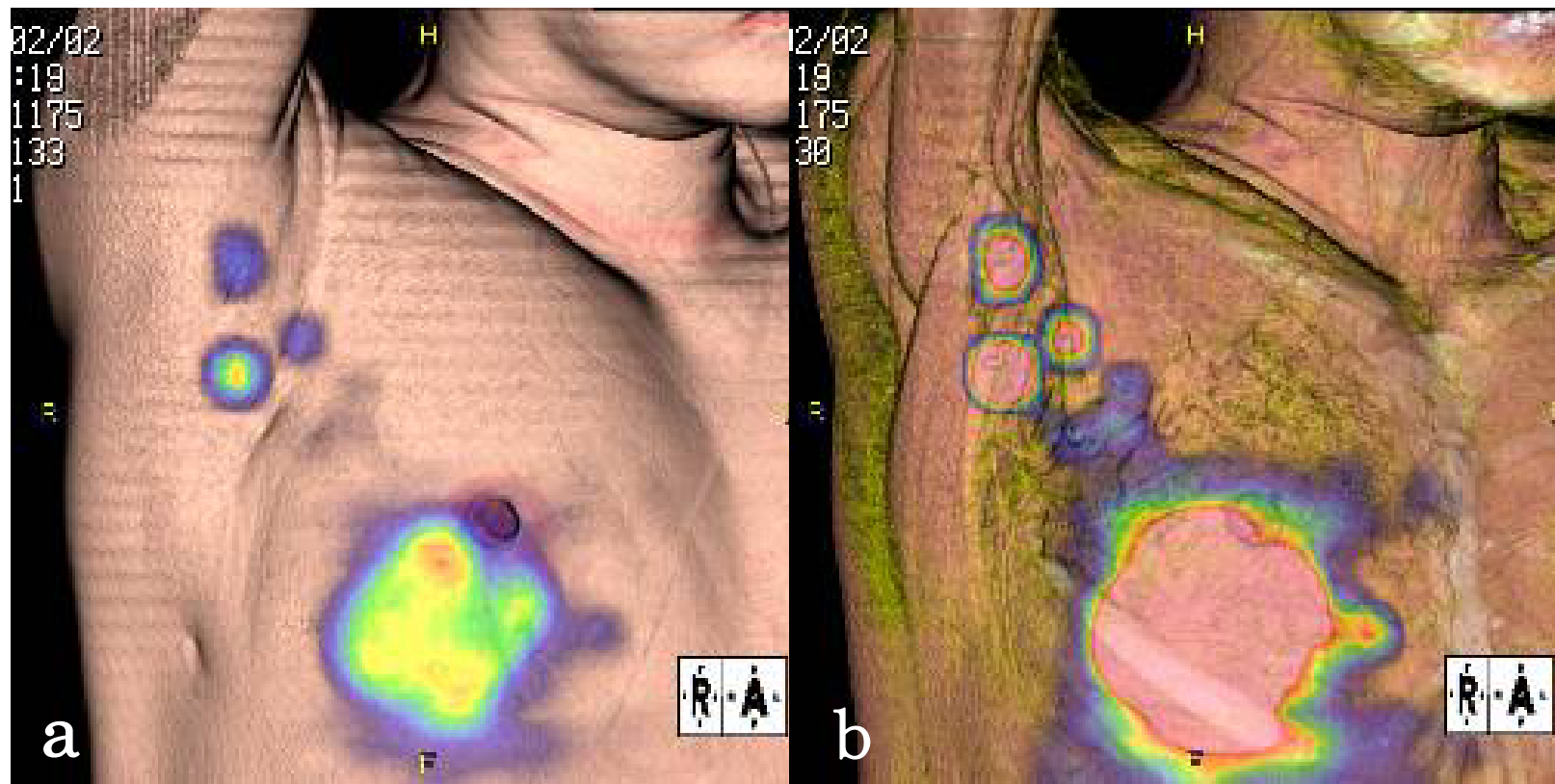


Fig.2



Fig.3

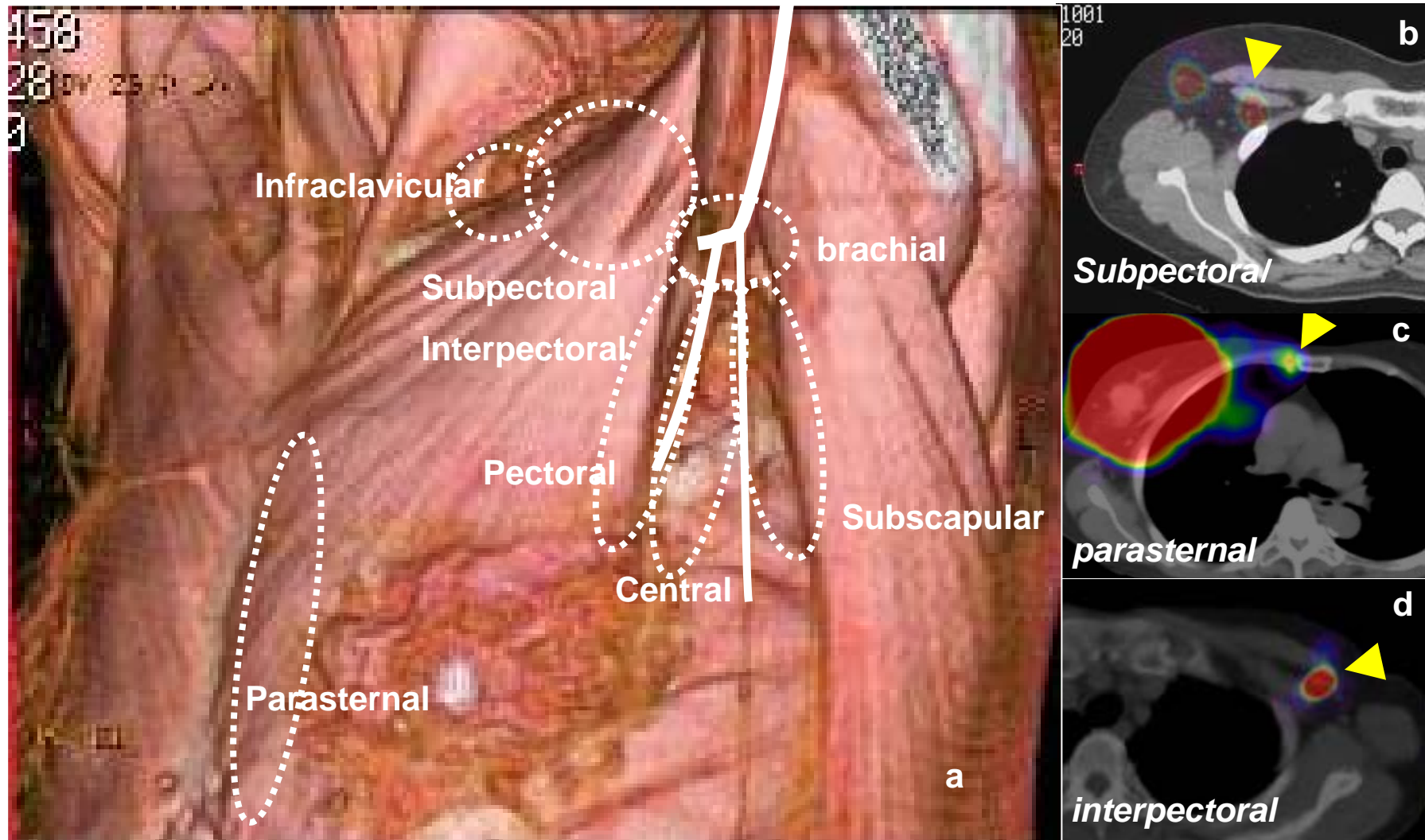


Fig.4

